

## Sol–Gel Derived Urea Cross-Linked Organically Modified Silicates. 2. Blue-Light Emission

L. D. Carlos,<sup>\*,†</sup> V. de Zea Bermudez,<sup>‡</sup> R. A. Sá Ferreira,<sup>†</sup> L. Marques,<sup>†</sup> and M. Assunção<sup>†</sup>

*Departamento de Física, Universidade de Aveiro, 3810 Aveiro, Portugal, and Secção de Química, Universidade de Trás-os Montes e Alto Douro, Quinta de Prados, Apartado 202, 5001 Vila Real Codex, Portugal*

*Received May 21, 1998. Revised Manuscript Received December 21, 1998*

The photoluminescence and the local structure of sol–gel derived organic–inorganic hybrids, so-called ureasils, are discussed. Their host matrix is a silica-based network to which different numbers of oxyethylene repeat units—8.5, 15.5, and 40.5 for U(600), U(900), and U(2000), respectively—are covalently grafted by means of urea linkages. The small-angle X-ray scattering (SAXS) results suggest a diphasic structure for the morphology of the hybrids induced by local phase separation between siliceous domains and polymeric regions. The estimated interdomain distances, ranging from 27 Å for U(600) to 59–64 Å for U(2000), indicate that the three ureasils are greatly homogeneous on the SAXS scale. The luminescence spectra show a broad light emission (2.0–4.1 eV) with a blue band at ~2.6 eV and a purplish-blue one at ~2.8–3.0 eV, clearly distinguished by time-resolved spectroscopy. The energies of these two components are related to the dimension of the backbone inorganic skeleton. The local structure of these amorphous siliceous regions is depicted as a planar structure that combines different proportions of six to eight silica-based chains (blue emission) with three to four organically modified Si–O environments (purplish-blue emission). The calculated coherent diffraction lengths of the siliceous domains for U(600), U(900), and U(2000)—16.6, 16.1, and 20.5 Å, respectively—points to an increase of the overall disorder of the inorganic backbone as the quantity of oxyethylene chains increase from 8.5 to 40.5.

### I. Introduction

Conductive complexes of high molecular weight polymers, such as poly(oxyethylene), POE, and poly(oxypropylene), POP, and metal salts have been the focus of intense investigations in the past 15 years<sup>1</sup> because of their various practical applications as high energy density batteries, sensors, and electrochromic and photoelectrochemical solid-state devices.<sup>1,2</sup>

More recently, luminescent polymer–salt complexes incorporating trivalent lanthanide cations in the open macromolecular host structure of POE and POP have drawn some interest as well.<sup>3–9</sup> Besides the potential

technological interest of these polymeric luminescent materials, the analysis of their luminescence spectra provides some insights on the characterization of their local ion-chain structures. In particular, the observed energies of POE–EuBr<sub>3</sub> have been used to determine the average Eu<sup>3+</sup>-nearest ligand distance,<sup>4,6</sup> the associated local symmetry group,<sup>4,6</sup> and the number and type of europium first neighbors.<sup>8</sup>

The encapsulation of luminescent centers into ligands protecting organic cage-type hosts (e.g., chelates and cryptates) is an area in which several efforts have been made in recent years, due to the possibility of obtaining stable supramolecular structures with potential applications in luminescent devices.<sup>10</sup> The absorption of ultraviolet light by the organic molecules and the subsequent emission, via an efficient intramolecular energy transfer to the emitter ion (antenna effect), are a remarkable characteristic of these materials. Unfortunately, despite the very attractive optical features of these cage-type materials, their poor thermal stability and mechanical

<sup>†</sup> Universidade de Aveiro.

<sup>‡</sup> Universidade de Trás-os Montes e Alto Douro.

(1) (a) *Polymer Electrolyte Reviews—1*; MacCallum, J. R., Vincent, C. A., Eds.; Elsevier Applied Science: London, 1987. (b) *Electrochemical Science and Technology of Polymers 1*; Linford, R. G., Ed.; Elsevier Applied Science: London, 1987. (c) *Polymer Electrolyte Reviews—2*; MacCallum, J. R., Vincent, C. A., Eds.; Elsevier Applied Science: London, 1989. (d) *Second International Symposium on Polymer Electrolytes*; Scrosati, B., Ed.; Elsevier Applied Science: London, 1990. (e) Gray, F. M. *Solid Polymer Electrolytes: Fundamentals and Technological Applications*; VCH: New York, 1991. (f) *Electrochemical Science and Technology of Polymers 2*; Linford, R. G., Ed.; Elsevier Applied Science: London, 1991.

(2) Armand, M. B. *Adv. Mater.* **1990**, *2*, 278.

(3) Huq, R.; Farrington, G. C. *Second International Symposium on Polymer Electrolytes*; Scrosati, B., Ed.; Elsevier Applied Science: London, 1990; p 273.

(4) (a) Carlos, L. D.; Assunção, M.; Abrantes, T. M.; Alcácer, L. *Solid State Ionics III*; Nazri, G.-A., Tarrascon, J.-M., Armand, M. B., Eds.; Materials Research Society Proceedings; MRS: Pittsburgh, PA, 1993; Vol. 293, p 117. (b) Carlos, L. D.; Videira, A. L. L. *Phys. Rev. B* **1994**, *49*, 11721. (c) Carlos, L. D.; Videira, A. L. L. *J. Chem. Phys.* **1994**, *101*, 8827.

(5) Brodin, A.; Mattsson, B.; Torell, L. *J. Chem. Phys.* **1994**, *101*, 4621.

(6) (a) Carlos, L. D.; Assunção, M.; Alcácer, L. *J. Mater. Res.* **1995**, *10*, 202. (b) Carlos, L. D.; Videira, A. L. L.; Assunção, M.; Alcácer, L. *Electrochim. Acta* **1995**, *40*, 2143.

(7) Di Noto, V.; Bettinelli, M.; Furlani, M.; Lavina, S.; Vidali, M. *Macromol. Chem. Phys.* **1996**, *197*, 257.

(8) (a) Videira, A. L. L.; Carlos, L. D. *J. Chem. Phys.* **1996**, *105*, 8878. (b) Carlos, L. D.; Videira, A. L. L. *Chem. Phys. Lett.* **1997**, *57*, 264.

(9) Ferry, A.; Furlani, M.; Franke, A.; Jacobsson, P.; Mellander, B.-E. *J. Chem. Phys.* **1998**, *109*, 2921.

(10) (a) Bredol, M.; Kynast, U.; Ronda, C. *Adv. Mater.* **1991**, *3*, 361. (b) Sabbatini, N.; Guardigli, M.; Lehn, J.-M. *Coord. Chem. Rev.* **1993**, *123*, 201.

properties have limited their use in either conventional phosphors or laser devices.

Furthermore, in the case of lanthanide-based POE cage-type luminescent materials, two very severe drawbacks were immediately recognized: (1) a strong tendency to crystallize, which reduces optical quality; (2) a high hygroscopic character, which enhances the quenching of the lanthanide emission by deactivations via O–H oscillators and makes handling in an inert atmosphere compulsory. To overcome these two problems and to improve both thermal stability and mechanical properties of the complexes, similar luminescent polymers based on organic–inorganic hybrids, so-called ormosils (organically modified silicates) or ormolytes (organically modified electrolytes), have been synthesized by the sol–gel process. The luminescent features of a series of Eu(III)-doped ormosils have been recently published.<sup>11–15</sup>

In particular, our group reported on the synthesis and general characterization (luminescent, thermal, and conducting properties) of a new class of luminescent ormosils doped with europium triflate.<sup>11,12</sup> These sol–gel derived hybrids are based on a siliceous network to which oligopolyoxyethylene chains are grafted by means of urea bridges and have been thus classed as ureasils (or ureasilicates).<sup>16</sup> The technological relevance of these europium-based ureasils may be foreseen. Apart from the fact that they are obtained as amorphous transparent monoliths, thermally stable up to 250 °C and exhibiting an ionic conductivity of about  $10^{-5} \Omega^{-1} \text{cm}^{-1}$  at 30 °C, these hybrids are multiwavelength phosphors (full-color or white-light emitters) combining narrow Eu<sup>3+</sup> yellow-red lines with a broad green-blue emission associated with the luminescence of the siliceous skeleton.<sup>11,12</sup>

The use of the sol–gel route for the synthesis of novel materials in many scientific fields is well-known.<sup>17</sup> It relies on the great versatility of the silicon chemistry resulting from the remarkable stability of Si–O and Si–C bonds. In addition, this chemical process possesses the following substantial advantages: (1) the high reactivity, purity, and homogeneity of the precursors; (2) the possibility of controlling the micro- and macro-

structure of the host matrix; (3) the presence of a siliceous network, which provides simultaneously good mechanical resistance, extraordinary thermal stability, and amorphous character; (4) the possibility of grafting organic groups to the inorganic backbone at low processing temperatures; (5) the possibility of preparing elastomeric transparent monoliths of variable thickness.<sup>17</sup>

Owing to the presence of its siliceous backbone skeleton, the undoped urea cross-linked organic–inorganic xerogels displayed broad visible luminescence spectra, between 14 K and room temperature, that appeared white to the eyes. These urea cross-linked ormosils are thus white-light phosphors even without the incorporation of any activator metal ion.<sup>11–13</sup> The achievement of full-color displays less expensive, more environmentally “friendly”, and which could replace with substantial advantages the currently used emissive centers is one of the main challenging tasks in the field of luminescent materials. A new class of stable and efficient white photoluminescent silicate materials prepared from an alkoxy silane (similar to the precursor used in the synthesis of the ureasils) and a carboxylic acid through a sol–gel route was recently reported.<sup>18</sup> When heated above ~400 °C, these hybrids display a short-lived luminescence ( $\leq 10$  ns) and a bright phosphorescence with a lifetime of several seconds at room temperature.<sup>18</sup>

Since the first experimental results focused on the bright-red photoluminescence of highly porous silicon layers,<sup>19</sup> a great deal of research effort has been devoted to understand and explore their visible-light emission features.<sup>20–26</sup> A lot of work has also been reported on light-emitting silicon-based materials with properties similar to those of porous silicon, such as organopolysilylene,<sup>26,27</sup> silicon clusters,<sup>28</sup> and siloxene-derived compounds.<sup>24–26</sup> These materials can be useful models for

(18) Green, W. H.; Le, K. P.; Grey, J.; Au, T. T.; Sailor M. J. *Science* **1997**, *276*, 1826.

(19) Canham, L. T. *Appl. Phys. Lett.* **1990**, *57*, 1046.

(20) (a) Cullis, A. G.; Canham, L. T.; Calcott, P. D. J. *J. Appl. Phys.* **1997**, *82*, 909. (b) Pifferi, A.; Taroni, P.; Torricelli, A.; Valentini, G.; Mutti, P.; Ghisloti, G.; Zanghieri, L. *Appl. Phys. Lett.* **1997**, *70*, 348.

(21) Canham, L. T.; Loni, A.; Calcott, P. D. J.; Simons, A. J.; Reeves, L.; Houlton, M. R.; Newey, J. P.; Nash, K. J.; Cox, T. I. *Thin Solid Films* **1996**, *276*, 112.

(22) Fauchet, P. M.; Peng, C.; Tsybeskov, L.; Vandyshev, J.; Dubois, A.; Raisanen, A.; Orłowski, T. E.; Brillson, L. J.; Fouquet, J. E.; Dexheimer, S. L.; Rehm, J. M.; McLendon, G. L.; Ettetdgui, E.; Gao, Y.; Seifert, F.; Kurinec, S. K. *Semiconductor Silicon/1994, 7th International Symposium on Silicon Materials Science and Technology*; Huff H. R., Bergholz, W., Sumino K., Eds.; Electrochemical Society Proceedings; The Electrochemical Society, Inc.: Pennington, NJ, 1994; Vol. 94-10, p 499.

(23) (a) Cameron, A.; Chen, X.; Trager-Cowan, C.; Uttamchandani, D.; O'Donnell, K. P. *Optical Properties of Low Dimensional Silicon Structures*; Bensahel, D. C., Canham, L. T., Ossicini, S., Eds.; Academic Press: Amsterdam, 1993.

(24) (a) Brandt, M. S.; Fuchs, H. D.; Stutzmann, M.; Weber, J.; Cardona, M. *Solid State Commun.* **1992**, *81*, 307. (b) Stutzmann, M.; Brandt, M. S.; Rosenbauer, M.; Weber, J.; Fuchs, H. D. *Phys. Rev. B* **1993**, *47*, 4806.

(25) Brus, L. *J. Phys. Chem.* **1994**, *98*, 3575.

(26) (a) Matsumoto, N. *Semiconductor Silicon/1994, 7th International Symposium on Silicon Materials Science and Technology*; Huff, H. R., Bergholz, W., Sumino, K., Eds.; Electrochemical Society Proceedings; The Electrochemical Society, Inc.: Pennington, NJ, 1994; Vol. 94-10, p 461. (b) Matsumoto, N.; Takeda, K.; Teramae, H.; Fujino, M. *International Topical Workshop on Advances in Silicon-Based Polymer Science, Hawaii, 1987*; Advances in Chemistry Series 224; American Chemical Society: Washington, DC, 1990. (c) Miller, R. D.; Michl, J. J. *J. Chem. Rev.* **1989**, *89*, 1359.

(27) Furukawa, K.; Fujino, M.; Matsumoto, N. *Macromolecules* **1990**, *22*, 1697.

(11) Carlos, L. D.; De Zea Bermudez, V.; Duarte, M. C.; Silva, M. M.; Silva, C. J.; Smith, M. J.; Assunção, M.; Alcácer, L. *Physics and Chemistry of Luminescent Materials VI*; Ronda, C., Welker, T., Eds.; Electrochemical Society Proceedings; The Electrochemical Society, Inc.: Pennington, NJ, 1998; Vol. 97–29, p 352.

(12) De Zea Bermudez, V.; Carlos, L. D.; Duarte, M. C.; Silva, M. M.; Silva, C. J.; Smith, M. J.; Assunção, M.; Alcácer, L. *J. Alloys Compd.* **1998**, *275–277*, 21.

(13) Ribeiro, J. L. S.; Dahmouche, K.; Ribeiro, C. A.; Santilli, C. V.; Pulcinelli, S. H. *J. Sol-Gel Sci. Technol.*, in press.

(14) Franville, A. C.; Zambon, D.; Mahiou, R.; Chou, S.; Troin, Y.; Coussens, J. C. *J. Alloys Compd.* **1998**, *275–277*, 831.

(15) (a) Jin, T.; Tsutsumi, S.; Machida, K.; Adachi, G. *J. Electrochem Soc.* **1996**, *143*, 3333. (b) Jin, T.; Inoue, S.; Tsutsumi, S.; Machida, K. *J. Non-Cryst. Solids* **1998**, *223*, 123.

(16) (a) Armand, M.; Poinsignon, C. J.; Sanchez, J.-Y.; De Zea Bermudez, V. French Patent 91 11349, 1991. (b) De Zea Bermudez, V.; Baril, D.; Sanchez, J.-Y.; Armand, M.; Poinsignon, C. J. *Optical Materials Technology for Energy Efficiency and Solar Conversion XI: Chromogenics for Smart Windows*; Hugot-Le Golf, A., Granqvist, C.-G., Lampert, C. M., Eds.; Proceedings SPIE, 1992; Vol. 1728, p 180.

(17) (a) *Sol–Gel Science and Technology*; Pope, E. J. A., Sakka, S., Klein, L. S., Eds.; Ceramic Transactions 55; The American Ceramic Society: Westerville, OH 1995. (b) Brinker, C. J.; Scherer, G. W. *Sol–Gel Science: The Physics and Chemistry of Sol–Gel Processing*; Academic Press: San Diego, CA, 1990. (c) Schmidt, H. *Chemistry, Spectroscopy and Applications of Sol–Gel Glasses*; Reisfeld, R., Jørgensen, C. K., Eds.; Springer-Verlag: Berlin, 1991; p 117.

understanding the structural properties of porous silicon. The establishment of the mechanisms leading to the photoluminescence and the development of light-emitting optical displays are two of the main research objectives. In addition, the luminescent features of porous silicon (or the luminescence of any other silicon-based material) might generate important developments in the interconnection between digital computing and digital communications, allowing the growth of optical communication devices directly on the silicon computer chip.<sup>25</sup> (Owing to its indirect infrared band gap, silicon itself cannot be used to generate communication optical signals.)

In the case of sol-gel derived silicate hosts, otherwise and notwithstanding the potential technological relevance of their optical properties,<sup>17,18,29-32</sup> only a limited amount of work has been focused on the light-emission features of the undoped gel itself.<sup>18,32,33</sup> The gel matrix has, in fact, basically been considered as an optically inert framework into which luminescent centers, such as lanthanide ions and organic dyes, can be incorporated.

The present work is the second of a series of two papers focused on the spectroscopic and local structure characterization of urea cross-linked organic-inorganic hybrids containing different numbers of oxyethylene units in their structure. The photoluminescence features of these white-light xerogels are presented and combined with X-ray diffraction and small-angle X-ray scattering data to discuss their local structure. Part 1 deals with the room-temperature mid-infrared spectroscopy.<sup>34</sup>

## II. Experimental Section

**Synthesis.** The hybrids analyzed in this work contain short, highly solvating oxyethylene units (CH<sub>2</sub>CH<sub>2</sub>O) covalently grafted onto the silica-based network by means of urea bridges. Their preparation has been described elsewhere.<sup>11,12,34</sup> The bond between the alkoxy silane precursor and the oligopolyoxyethylene segment is formed by the reaction of amine with isocyanates in tetrahydrofuran (THF), which leads to the formation of urea bonds. The terminal amino groups of doubly functional amines— $\alpha,\omega$ -diaminopoly(oxyethylene-co-oxypropylene)—were reacted with 3-isocyanatopropyltriethoxysilane, ICPTES. The grafting process was infrared-monitored: as the reaction proceeds, the very strong and sharp absorption band at about 2274 cm<sup>-1</sup>, attributed to the vibration of the  $\equiv\text{Si}(\text{CH}_2)_3\text{NCO}$  group, progressively decreases, while bands due to the presence of urea groups increase. The three diamines used are commercially designated as Jeffamine ED-2001 (~40.5 repeat units), Jeffamine ED-900 (~15.5 repeat units), and Jeffamine ED-600 (~8.5 repeat units). The ureasils will

be identified by the designation U(Y), where U originates from the word "urea" and Y = 600, 900, or 2000, indirectly indicating the length of the oligopolyoxyethylene chains.

**Materials and Methods.** Jeffamine ED-2001 (Fluka) was dried under vacuum at 90 °C for several days prior to being used. Jeffamine ED-600 (Fluka), Jeffamine ED-900 (Fluka), ICPTES, THF (Merck), and poly(ethylene glycol), PEG (average molecular weight of 2000, Aldrich) were utilized as purchased.

X-ray diffraction patterns were recorded using a Rigaku Geigerflex D/max-c diffractometer system. The films were exposed to the Cu K $\alpha$  radiation ( $\lambda = 1.54 \text{ \AA}$ ) at room temperature in a  $2\theta$  range (scattering angle) between 4 and 80°.

Small-angle X-ray scattering measurements were performed in a X'Pert Philips MPD system (PW3373/00 Cu LFF X-ray tube) using the Cu K $\alpha$  radiation. All SAXS data were not treated to remove any background component like parasitic scattering and thermal density fluctuations. The SAXS curves are displayed in a plot of intensity  $I(q)$  versus the scattering vector  $q$  ( $q = 4\pi\lambda^{-1} \sin \theta$ ). The analysis of the SAXS scattering profiles will be essentially focused on the discussion of local phase separation between the inorganic-rich domains and the polymeric chains.

The luminescence spectra were obtained using a 0.25 m excitation monochromator (KRATOS GM-252)—fitted with a 1180 grooves/mm grating blazed at 240 nm—and a 1 m spectrometer (1704 SPEX Czerny-Turner)—fitted with a 1200 grooves/mm grating blazed at 500 nm—coupled to a photomultiplier (RCA C31034). The spectra were collected at 90° between 14 and 310 K, with a resolution of about 0.05 nm. The light source was a 1000 W Xe arc lamp (KRATOS LH 15 IN/1 S).

The time-resolved luminescence spectra were carried out at 14 K using a pulsed Xe arc lamp with a pulse width of 3  $\mu\text{s}$  as the light source (tail after 10  $\mu\text{s}$  accounts for 1% of initial intensity) and a phosphorimeter (SPEX 1934 C).

## III. Results

**Powder X-ray Diffraction.** The room-temperature X-ray diffraction patterns of U(600), U(900), and U(2000) are depicted in Figure 1. The diffraction patterns of U(600) and U(900) show a broad hump centered at 21.20° and 20.36°, respectively, associated with the presence of amorphous siliceous domains.<sup>35,36</sup> For U(900), this band, which is shifted toward smaller angles, is broader and its intensity is half-reduced. In addition, the weak hump, seen in U(600) at around 40–45°, is not clearly observed. The polymer chains are essentially in a disordered regime as pointed out by the absence of crystalline oligomeric regions. All these features point to an increase of the overall disorder of the siliceous skeleton (small coherent domains) as the quantity of incorporated oxyethylene moieties increases from 8.5 in U(600) to 15.5 in U(900).

The U(2000) X-ray spectrum is dominated by the presence of two intense well-defined Bragg peaks at 19.15° and 23.25°. As can be concluded from the inset of Figure 1, these peaks are associated with the diffraction of crystalline PEG (which contains about 40.5 oxyethylene repeat units, similar to the number of units present in the structural formula of the U(2000) hybrid).

(28) (a) Furukawa, K.; Fujino, M.; Matsumoto, N. *Appl. Phys. Lett.* **1992**, *60*, 2744. (b) Heath, J. R. *Science* **1992**, *258*, 1131.

(29) (a) Reisfeld, R. *J. Non-Cryst. Solids* **1990**, *121*, 254. (b) Camostrini, R.; Carturan, G.; Ferrari, M.; Montagna, M.; Pilla, O. *J. Mater. Res.* **1992**, *7*, 745. (c) Costa, V. C.; Lochhead, M. J.; Bray, K. L. *Chem. Mater.* **1996**, *8*, 783.

(30) (a) Reisfeld, R. *Sol-Gel Science and Technology*; Aegerter, M. A., Jafellicci, J. M., Souza, J. F., Zanutto, E. D., Eds.; World Scientific: Singapore, 1989; p 323. (b) Reisfeld, R.; Jørgensen, C. K. *Chemistry, Spectroscopy and Applications of Sol-Gel Glasses*; Reisfeld, R., Jørgensen, C. K., Eds.; Springer-Verlag: Berlin, 1991; p 207. (c) Luther-Davies, B.; Lochhead, M. J.; Bray, K. L. *Chem. Mater.* **1996**, *8*, 2586.

(31) Judeinstein, P.; Sanchez, C. *J. Mater. Chem.* **1996**, *6*, 511.

(32) Zaitoun, M. A.; Kim, T.; Lin, C. T. *J. Phys. Chem. B* **1998**, *102*, 1122.

(33) García, M. J.; Mondragón, M. A.; Téllez, C. S.; Campero, A.; Castaño, V. M. *Mater. Chem. Phys.* **1995**, *15*, 41.

(34) De Zea Bermudez, V.; Carlos, L. D.; Alcácer, L. **1999**, *3*, xxx.

(35) (a) West, A. R. *Solid State Chemistry and its Applications*; John Wiley & Sons: New York, 1984; p 606. (b) Giacomazzo, C.; Monaco, H. L.; Viterbo, D.; Scordari, F.; Gilli, G.; Zanotti, G.; Catti, M. *Fundamentals of Crystallography*; Oxford Science Publications: New York, 1995; p 213.

(36) Moss, S. C. In *Physics of Disorder Materials*; Adler, D.; Fritzsche, H.; Ovshinsky, S., Eds.; Plenum Press: New York, 1985.



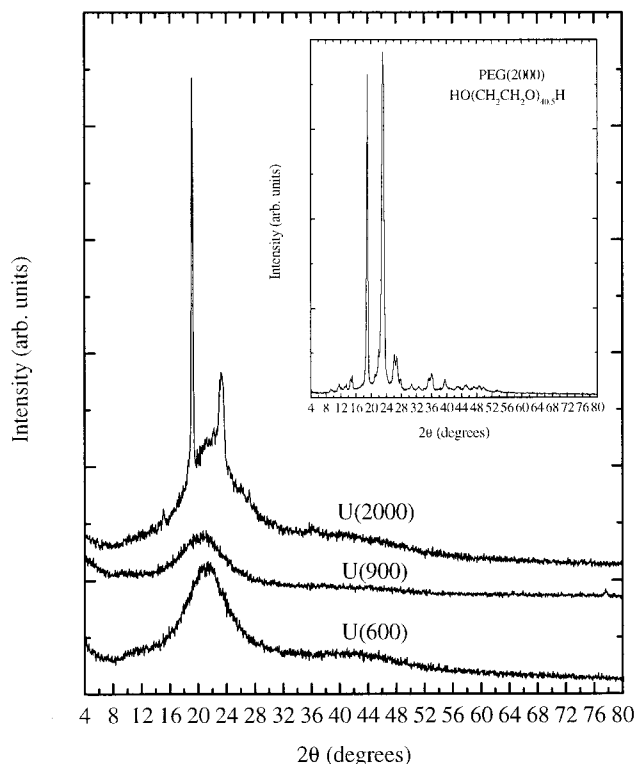


**Figure 1.** X-ray diffraction patterns for U(600), U(900), and U(2000). The inset shows the X-ray spectrum of a low molecular weight poly(ethylene glycol), PEG.

This polymer is a low molecular weight POE. Although the position of the two Bragg peaks in U(2000) is almost the same as that of the corresponding peaks for pure PEG, there is a relative intensity inversion (approximately by a factor of 2), probably related to changes in the conformation of the polymer chains after their incorporation into the ureasil structure. This is confirmed by infrared data.<sup>34</sup> The amorphous band and the weak hump are also distinguished in the U(2000) diffraction pattern centered around 21.61° and 40–45°, respectively.

To attempt an estimation of the position of the amorphous siliceous band and of its full width at half-maximum (fwhm), the X-ray patterns of the three hybrids are fitted to Gaussian-type functions. For U(2000) the two PEG Bragg peaks have been taken explicitly into account (also as Gaussian-type functions) in the fit because of their superposition with the broad band.

For amorphous solids, the position of the first sharp diffraction peak (FSDP) can be related, via a reciprocal relation, to a distance in the real space between the structural units (Bragg law).<sup>36,37</sup> The Scherrer equation,<sup>37</sup>  $fwhm = (0.94\lambda)/(L \cos \theta)$  (fwhm in radians), has been used to estimate a coherent length  $L$  over which the structural unit survives.<sup>36,37</sup>

Using the experimental FSDP positions, structural unit distances of 4.2, 4.4, and 4.1 Å have been obtained for U(600), U(900), and U(2000), respectively. These values are similar to those reported for vitreous SiO<sub>2</sub>, i.e., 4.2 Å.<sup>35,36</sup> This structural unit distance is larger

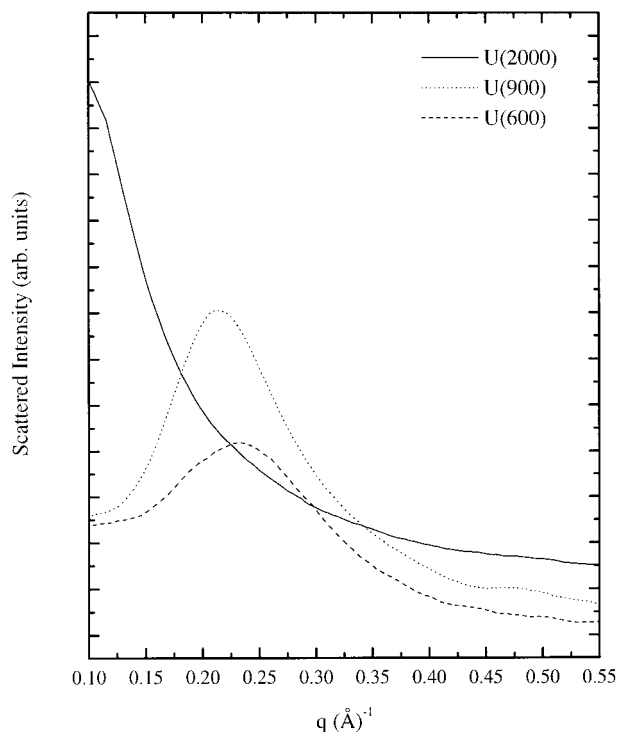


**Figure 2.** SAXS scattering profiles for U(600) (dash line), U(900) (dot line), and U(2000) (full line).

than the Si–O, O–O, and Si–Si distances, equal to 1.62, 2.65, and 3.12 Å, respectively, and represents the buildup of correlations whose basic period is well beyond the first few near-neighbor distances.<sup>36</sup> In accordance with those conclusions, the structural unit distances calculated above for the three ureasils will also reflect a local order that is developed over distances beyond the first few shells of neighbors.

The coherent lengths calculated by the Scherrer relation are 16.6, 16.1, and 20.5 Å for U(600), U(900), and U(2000), respectively. These values are identical to the one reported—using small-angle X-ray scattering—for the diameters of the siliceous domains in organically modified silicates similar to the ureasils described here.<sup>38</sup> Taking the ratio between the coherent length and the structural unit distance, the average number of structural units present in each diameter of the coherent diffracting domains of each hybrid has been estimated to be approximately 4.0 for U(600), 3.7 for U(900), and 5.0 for U(2000).

**SAXS Scattering.** Figure 2 presents the SAXS curves of U(600), U(900), and U(2000). These scattering profiles display a single interference peak indicative of a nonhighly periodic fluctuation of the electron density within the ureasils. This result suggests a diphasic structure for the morphology of the hybrids caused by local phase separation between inorganic silicon-rich domains and polymeric regions. As can be seen from Figure 2, the maximum scattering intensity and the interdomain spacing  $d$  ( $d = 2\pi/q$  where  $q$  is the magnitude of the scattering vector of the peak maximum) increase with the increase of the length of the oligopolyoxyethylene chains. These results, also observed in related ormolytes based on tetraethoxysilane,

(37) (a) Guinier, A. *X-ray Diffraction in Crystals, Imperfect Crystals and Amorphous Bodies*; Dover: New York, 1994. (b) Warren, B. E. *X-ray Diffraction*; Adisson Wesley: New York, 1969.

(38) Rousseau, F.; Poinsignon, C.; Garcia, J.; Popall, M. *Chem. Mater.* **1995**, *7*, 828.

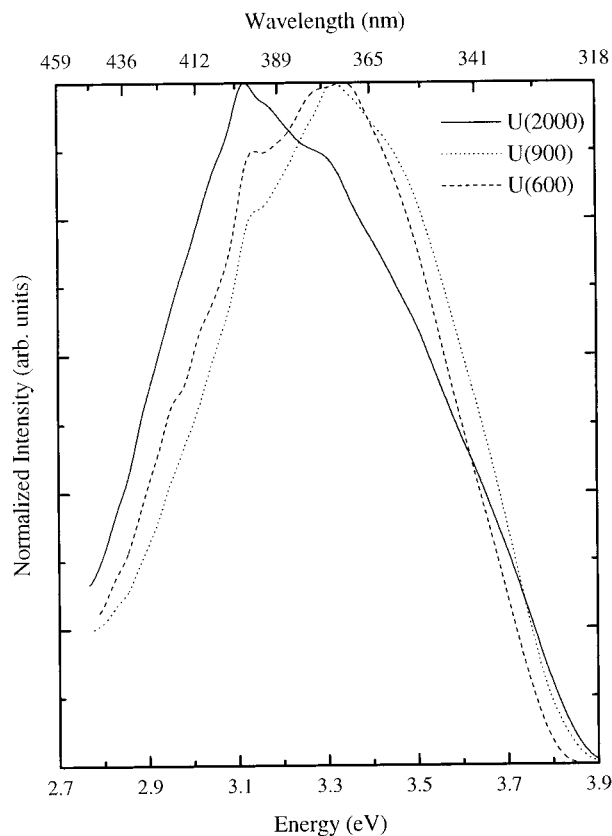


**Figure 3.** Excitation spectra,  $\lambda_{\text{emiss}} = 462$  nm (2.68 eV), for U(600) (dash line), U(900) (dot line), and U(2000) (full line) at 14 K. The intensities are proportional to the photon flux and are normalized to the most intense peak in each spectrum.

TEOS, and PEG<sup>39</sup> and organic–inorganic network ceramers,<sup>40</sup> support the suggestion that the peak is due to interparticle scattering interference, since an increase of the polymer chain's end-to-end distance would cause the inorganic-rich domains to be spaced further apart from each other.<sup>39,40</sup> From the magnitude of the scattering vector  $q$  of the peak maximum, Figure 2, we estimate the corresponding interdomain distances  $d$  for the three ureasils as 27.1 for U(600), 29.1 for U(900), and 59–64 Å for U(2000).

These correlation lengths indicate a great homogeneity on the SAXS scale for the ureasil hybrids. In fact, although these distances are much smaller than the values reported for other similar ormosils,<sup>38–42</sup> the estimated interdomain values for U(600) and U(900) are of the same order of magnitude than the ones observed for organic–inorganic composites based on mixtures of TEOS with diethylene and tetraethylene glycol<sup>39</sup> and based on mixtures of TEOS and tetramethoxysilane, TMOS, with poly(methyl methacrylate-*co*-[3-(methacryloxy)propyl]trimethoxysilane), PMMSi.<sup>42</sup>

This model for the ureasils morphology based on a diphasic structure induced by local phase separation between inorganic modified silica-based domains and

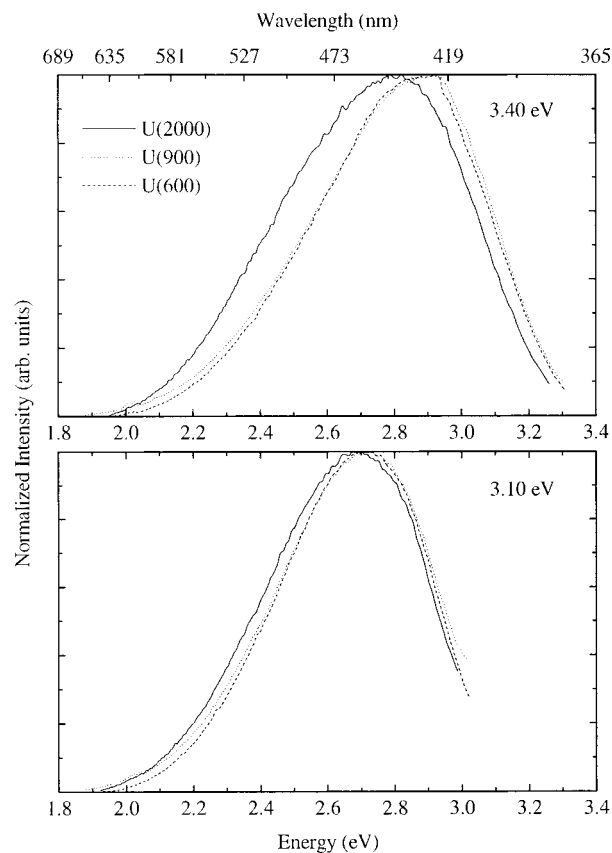


**Figure 4.** Emission spectra for U(600) (dash line), U(900) (dot line), and U(2000) (full line) for two different excitation energies at 14 K: (top) 3.40 eV; (bottom) 3.10 eV.

organic-rich regions is similar to models proposed for other classes of hybrid materials, such as related ormosils based on TEOS and PEG<sup>39</sup> and organic–inorganic network ceramers.<sup>40</sup>

**Photoluminescence and Time-Resolved Spectroscopy.** The excitation spectra, recorded at 2.68 eV (462 nm) of U(600), U(900), and U(2000) at 14 K exhibit a large broad band between 2.76 and 3.94 eV (315 and 450 nm) as shown in Figure 3. Two different unshaped peaks are clearly distinguished and are centered around 3.31–3.32 and 3.12–3.14 eV (374–375 and 395–398 nm). Although the energies of the peaks for U(600) and U(900) are approximately the same, the latter hybrid excitation band is broader and there is a decrease in the relative intensity of its 3.14 eV (395 nm) peak. In addition, as the number of oxyethylene repeat units is increased from approximately 15.5 in U(900) to 40.5 in U(2000), the excitation spectrum shifts toward lower energies (red shift). Simultaneously, an intensity inversion between the two peaks is observed.

The emission spectra of U(600), U(900), and U(2000) excited by photons of 3.40 eV (365 nm) and 3.10 eV (400 nm) at 14 K are shown in Figure 4. The emission band is very broad and Gaussian in shape. For the entire range of excitation energies used, 2.95–3.54 eV, no significant differences are detected between the U(600) and the U(900) luminescence, namely, in the high-energy region (above 2.5 eV). Upon inclusion of more 25 oxyethylene moieties, the U(2000) emission is shifted to the red, in accordance with the corresponding red shift of the U(600) and U(900) excitation spectra mentioned above (Figure 3). As the excitation energy

(39) Judeinstein, P.; Titman, J.; Stamm, M.; Schmidt, H. *Chem. Mater.* **1994**, *6*, 127.

(40) Rodrigues, D. E.; Brennan, A. B.; Betrabet, C.; Wang, B.; Wilkes, G. L. *Chem. Mater.* **1992**, *4*, 1437.

(41) Sanchez, C.; In, M. *J. Non-Cryst. Solids* **1992**, *147*, 1.

(42) Coltrain, B. K.; Landry, C. J. T.; O'Reilly, J. M. O.; Chamberlain, A. M.; Rakes, G. A.; Sedita, J. S.; Kelts, L. W.; Landry, M. R.; Long, V. K. *Chem. Mater.* **1993**, *5*, 1445.

decreases from 3.54 to 2.95 eV (350–420 nm), the red shift is reduced approximately by an order of magnitude from 0.1 to 0.01 eV and the U(2000) emission spectrum resembles those of the other two ureasils, namely, for higher energies. For the low-energy region of the spectra, however, only slight differences between the photoluminescence of the three organic–inorganic matrices persist. These differences are still observed for U(600) and U(900) over all the excitation energies used. No intensity degradation under UV radiation was observed, and as temperature rises from 14 to 310 K, the ureasils emission intensity is generally reduced by 30–40%.

It is well established that silicon-based materials, such as porous silicon,<sup>19–25</sup> organopolysilylene,<sup>26,27</sup> silicon clusters,<sup>28</sup> siloxene-derived compounds,<sup>24–26</sup> silica gels,<sup>29,30,32</sup> and TEOS<sup>33</sup> (one of the mostly used sol–gel precursor), can emit light within a wide energy region ranging from ultraviolet to infrared.<sup>22,26</sup> The dimensional hierarchy of their backbone silicon-based structures determines the emission energy in such a way that an increase in the siliceous network dimension results in a decrease of the corresponding energy gap.<sup>26,43</sup> Moreover, there is strong evidence that a blue emission is essentially oxide-related.<sup>18,21–24,33,43</sup> Therefore, the observed broad luminescence of the organic–inorganic modified silicates described here certainly originates from the presence of a siliceous backbone skeleton (with spatial inhomogeneities, according to the observed broadening).

In an attempt to gain some insight about the emission energies and the corresponding local structure of the ureasils, a deconvolution of their broad emission was performed. For excitation energies between 3.10 and 3.54 eV (350–400 nm), the deconvolution curve-fitting procedure reveals the presence of two unshaped Gaussian bands in the blue (~2.6 eV) and purplish-blue (~2.8–3.0 eV) spectral regions. This latter component is not observed for excitation energies lower than 2.95 eV (420 nm). The following procedure was used to fit the experimental emission spectra to the Gaussian parameters (peak energy, integrated intensity, and fwhm). First, one Gaussian function was adjusted to fit the single-blue hybrids emission excited at 2.95 eV. Since the fwhm is determined primarily by carrier–phonon interaction, its value is not affected by changes in the excitation energy.<sup>44</sup> Therefore, for each ureasil, the blue and purplish-blue fwhm-fitted values were considered to be independent of the excitation energy. In contrast, the peak energies and their integrated intensity were, for each hybrid, free to vary for the whole excitation energy range used. Second, taking into account the calculated fwhm for the blue band, two Gaussian functions were adjusted to fit all the other emissions in such a way that unambiguous curve-fit results could be obtained, imposing a constant value for the fwhm of the purplish-blue component. The calculated relative integrated intensities of the two bands indicate that for U(2000) the contribution of the blue component is larger than the purplish-blue one, whereas

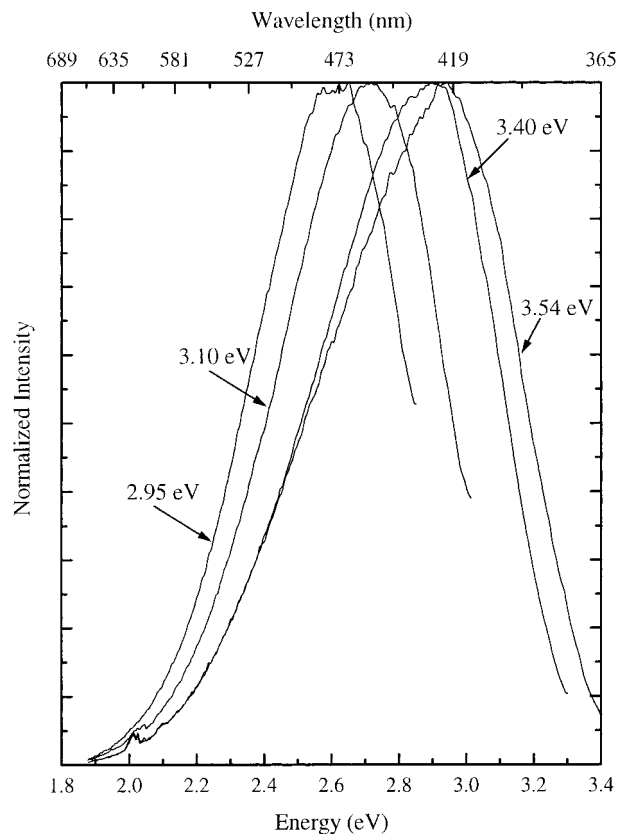


**Figure 5.** Emission spectra for U(900) at 14 K using different excitation energies. The spectra have been scaled to the same peak height for easier comparison.

for the other two ureasils the emission spectra are dominated by the latter contribution.

When the excitation energy is decreased from 3.54 to 2.95 eV, the ureasil's broad emission is strongly shifted to the red, as illustrated in Figure 5 for U(900). This red shift, which has been reported for other silicon-based materials,<sup>24,44,45</sup> is also clearly evidenced in the luminescence excitation recorded for different emission wavelengths, shown in Figure 6 for U(600). Although the excitation of luminescence in the blue region (2.71–2.61 eV, 458–475 nm) occurs mainly via the sharp peak centered at 3.12–3.14 eV (395–398 nm), emission in the purplish-blue region (2.83–2.79 eV, 438–445 nm) is excited predominantly through the broad band around 3.40 eV (365 nm). Since the maximum intensity of the excitation spectra of U(600) and U(900) is found at approximately 3.40 eV, their broad emission bands have a greater contribution of the purplish-blue component, unlike U(2000) for which the maximum intensity of the excitation spectra is observed around 3.12 eV and whose luminescence is dominated by the blue emission. Since in the U(900) excitation spectrum the relative intensity of the 3.14 eV peak is lower than that observed for U(600) (Figure 3), the contribution of the blue band for the U(900) emission is inferior. The same conclusions can be drawn from the variation of the integrated intensity of each band with the excitation energy calculated from the deconvolution of the different spectra.

(43) Konstantinov, A. O.; Henry, A.; Harris, C. I.; Janzén, E. *Appl. Phys. Lett.* **1995**, *66*, 2250.

(44) (a) Street, R. A. *Adv. Phys.* **1981**, *30*, 593. (b) Shah, J.; Pinczuk, A.; Alexander, F. B.; Bagley, B. G. *Solid State Commun.* **1982**, *42*, 717.

(45) (a) Munekata, H.; Murasato, S.; Kokimoto, H. *Appl. Phys. Lett.* **1980**, *37*, 536. (b) Chen, W.-C.; Feldman, B. J.; Bajaj, J.; Tong, F.-M.; Wong, G. K. *Solid State Commun.* **1981**, *38*, 357.

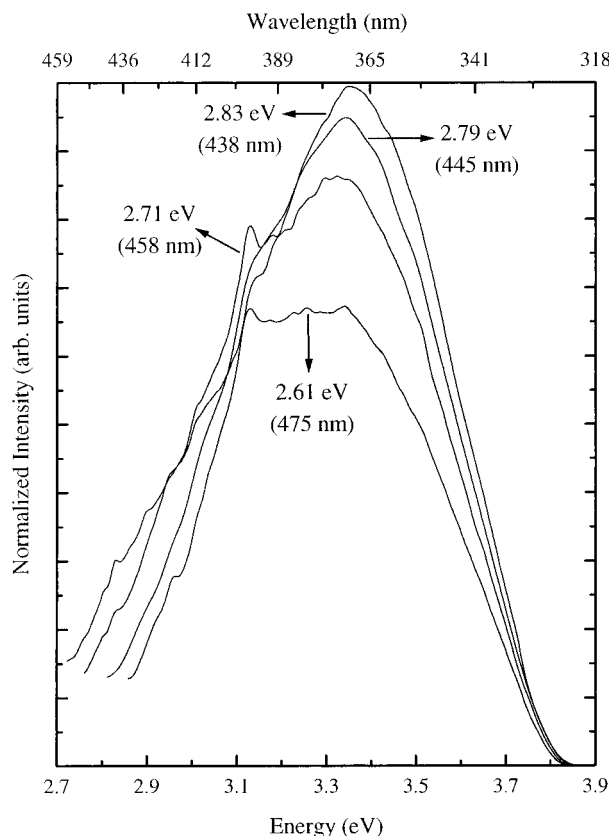


**Figure 6.** Excitation spectra for U(600) at 14 K using different emission energies.

The coexistence of the blue and purplish-blue components in the ureasils emission could be clearly illustrated in the time-resolved spectra presented for U(600) in Figure 7. At short delay times, between 1 and 5 ms, the higher-energy purplish-blue component is distinctly observed. However, with increasing delay time, the intensity of this band decreases, and at delays longer than 10 ms the spectra only display the longer-lived blue emission. Besides the evidence of the coexistence of these two bands, these results also indicate different lifetimes for the electron-hole recombination mechanisms that must be the origin of the observed luminescence.

#### IV. Discussion

The red shift observed in the ureasils emission with the decrease of the excitation energy (Figure 5) may be interpreted in terms of photoexcitation above a "thermalization gap".<sup>44,45</sup> The charge carriers photoexcited at energies greater than this "thermalization gap" relax always to the same energy levels before recombining. For photons of lower energies, a significant number of electrons and holes can be photoexcited to states below this gap (so-called localized band-tail states), where they will recombine radiatively with an energy shifted toward the red. The decrease of the calculated purplish-blue energies with the diminution of the excitation energy (from 3.0 to 2.8 eV), contrary to the case of the blue component, that is almost photoexcitation independent, suggests the possible existence of a "thermalization gap" for the purplish-blue emission.

As stated above, the emission energy of silicon-based materials depends on the hierarchy of their backbone

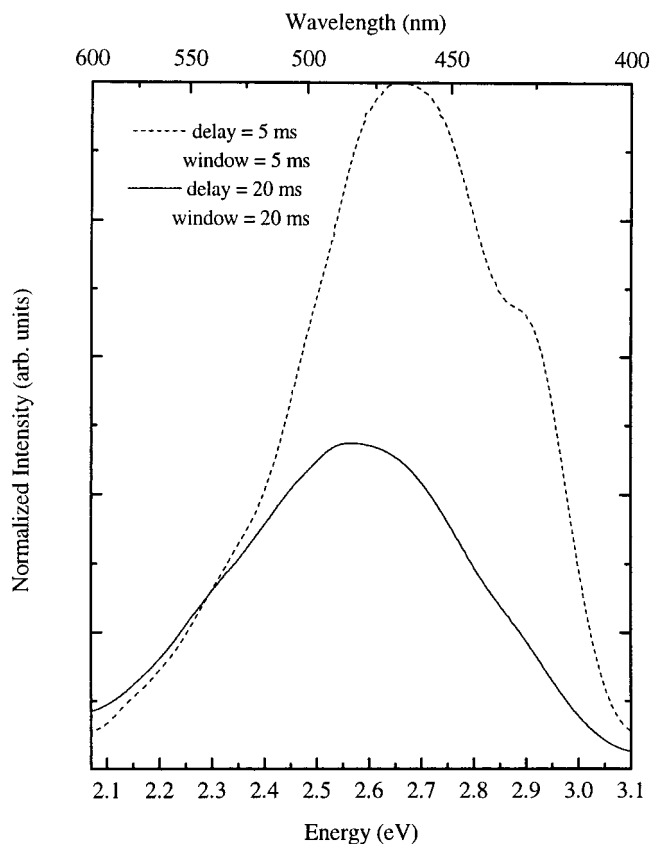


**Figure 7.** Time-resolved spectra for U(600) at 14 K,  $\lambda_{\text{emiss}} = 365$  nm (3.40 eV), using two different delay times and acquisition windows: 5 ms (dash line) and 20 ms (full line).

dimensions. As the network dimension increases from zero to three, the band gap energies change systematically from 6.5 to 1.1 eV.<sup>26</sup> This dependence of the energy gap on the backbone dimensions is related to the extension of the silicon  $\sigma$ -conjugations along the network. These  $\sigma$ -conjugations induce the electrons' delocalization with the corresponding formation of electronic band structures. Increases in their extension along the silicon backbone induce a decrease in the energy gap values with the corresponding increase in the skeleton dimensions. Despite its simplicity, this model has been used to obtain a quantitative connection between gap energies and local structure dimensions in silicon-based materials.<sup>26</sup> Also, in porous carbide samples the observed emission spectra show a more prominent high-energy component as the fiber size is reduced.<sup>43</sup> This connection will be employed next to relate the emission energies of the three ureasils described here to the structure of their inorganic skeleton.

Employing the quantitative dependence of band gap energies on network unit members derived by Matsuzono,<sup>26</sup> we suggest that the low-energy blue emission value ( $\sim 2.6$  eV) may correspond to a series of approximately six to eight silica-based chains, whereas the high-energy purplish-blue emission ( $\sim 2.8$ – $3.0$  eV) may be associated with a different series of approximately three to four siliceous skeleton units. Moreover, the energy values observed for both blue and purplish-blue bands could be an indication that the hybrid's inorganic structure is essentially a two-dimensional network, similar to the case of another class of organically modified electrolytes (classed as aminosils) whose struc-



ture is thought to be a ladder polymer based on a two-dimensional silicate network.<sup>46</sup>

Two different inorganic-rich regimes involving these two siliceous local structures can be considered in the depiction of their morphology. Although they can exist independently in different spatial regions of the ureasil's structure, the morphology of the coherent diffracting domains may be depicted as a mixture of the two kinds of siliceous local structures (the blue and the purplish-blue one). As the quantity of poly(oxyethylene) chains increases from 8.5 for U(600) to 40.5 for U(2000), the relative proportion between these two types of local siliceous arrangements will change (as the calculated integrated intensities point out) and, consequently, the length of the coherent domains of each hybrid is altered, as indicated by the X-ray results.

It is interesting to note that this description of the differences between the local structure of the three hybrids (as the number of oxyethylene units is increased from 8.5 to 40.5) in terms of a more efficient local phase separation (associated with an increase of the interdomain spacing and of the number of blue chains) agrees very well with similar observations reported for the emission spectra of aged and fresh TEOS.<sup>33</sup> In this case, the marked differences observed between the emission of aged and fresh TEOS (a red shift of the former spectrum) have been attributed to the presence of oligomers of higher molecular weight in the aged sample.

The red shift observed in the emission spectra of Figure 4 as the number of polymer chains increases from U(900) to U(2000) may also be interpreted in terms of the existence, in the structure of the ureasils, of different amounts of the two types of local siliceous environments. As mentioned above, the inorganic component of the U(2000) host is composed mainly of silica-based blue domains, whereas U(600) and U(900) have a larger amount of siliceous purplish-blue regions. For excitation energies that predominantly excite these latter regions (3.54–3.40 eV), the integrated intensity of their emissions in U(600) and U(900) is larger than the ones associated with the blue domains. For U(2000), on the other hand, the values of the blue integrated intensities are always larger and, therefore, their emission spectra are shifted toward the red. When the excitation energy decreases, the purplish-blue integrated intensities become similar for the three hybrids and no significant differences are detected between the maximum position of the emission spectra of the three hybrids.

As in the case of the silicon-based materials mentioned above, electron–hole recombination processes involving strongly correlated electron–hole exciton states or radiative tunneling between localized states of the electrons and holes may be the mechanisms that, occurring in the ureasil siliceous backbone, are the cause of the observed emission.<sup>20,23,24</sup> However, in what concerns the luminescent species responsible for that blue/purplish-blue emission, we are at this stage unable to perform a precise identification. An eventual contribution from the C=O and N–H groups of the urea cross-linkages to the observed long lifetimes could not be

refused. In fact, it is possible that the emission of the ureasil hybrids could arise from emitter species involving the urea bridges and the siliceous domains. An analogous luminescent center formed by a carbonyl group trapped on a Si–O–Si network was recently considered as being responsible for the photoluminescence of silicate–carboxylate sol–gel hybrids<sup>18</sup> and for the blue emission of oxidized porous silicon<sup>21</sup> and oxidized silicon carbides.<sup>43</sup>

## V. Conclusions

The photoluminescence spectra of the three sol–gel derived hybrids exhibit light emission between 2.0 and 4.1 eV whose deconvolution shows two unshaped Gaussian bands in the blue (~2.6 eV) and purplish-blue (~2.8–3.0 eV) spectral regions. Owing to the different time dependence of the recombination electron–hole mechanisms that may be the cause of these two bands, they are distinctly observed by time-resolved spectroscopy. The lower energy blue emission (slower component) is connected to larger local environments approximately ascribed to a series of six to eight connecting silica-based chains. The higher energy purplish-blue emission (faster component), on the other hand, is associated with smaller arrangements of approximately three to four siliceous units. In each one of the three ureasils the inorganic coherent domains combine different proportions of both kinds of silicon-based local structures. The energy values observed for the ureasils emission may suggest a two-dimensional network for their inorganic structure, as in the case of similar organically modified electrolytes (aminosils).

The SAXS scattering results indicate a diphasic structure for these ureasils in which the planar siliceous domains (composed of a mixture of the two different local environments) are separated from each other by organic oligomeric regimes and/or by organic–inorganic mixed regions. The estimated interdomain distances, 27.1 for U(600), 29.1 for U(900), and 59–64 Å for U(2000), indicate that these hybrids are greatly homogeneous on the SAXS scale.

The X-ray diffraction results indicate an increase of the overall disorder of the inorganic backbone as the quantity of incorporated oxyethylene moieties increases from 8.5 for U(600) to 15.5 for U(900). For the U(2000) hybrid, however, the siliceous coherent domains are clearly larger. By use of the experimental value of the position of the amorphous first diffraction peak and its full width at half-maximum, average structural unit distances of 4.2, 4.4, and 4.1 Å and coherent diffraction lengths of 16.6, 16.1, and 20.5 Å were obtained for U(600), U(900), and U(2000), respectively. Taking into account the ratio between the coherent length and the unit distance values, the average number of structural units per diameter of each coherent diffracting domain has been estimated to be approximately 4.0, 3.7, and 5.0 for U(600), U(900), and U(2000), respectively.

**Acknowledgment.** The authors thank L. Rino and P. Ventura of the Physics Department of University of Aveiro for fruitful comments on the luminescence analysis. The financial support provided by the Fundação para a Ciência e Tecnologia, FCT, (PBIC/CTM/1965/95) is gratefully acknowledged.

CM980373N

(46) (a) Charbouillot, Y.; Ravaine, D.; Armand, M. B.; Poinsignon, C. *J. Non-Cryst. Solids*. **1988**, *103*, 325. (b) Schubert, U.; Hüsing, N.; Lorenz, A. *Chem. Mater.* **1995**, *7*, 2010.